

# Modeling of $\text{Cr}^{3+}$ doped KZnCST Single Crystals

Maroj Bharati<sup>a</sup>, Vikram Singh<sup>a</sup>, Ram Kripal<sup>b</sup>

<sup>a</sup>Department of Physics, Nehru Gram Bharti (DU), Jamunipur, Prayagraj, India

<sup>b</sup>EPR Laboratory, Department of Physics, University of Allahabad, Prayagraj-211002, India

Tel: 91-532-2470532; Fax: 91-532-2460993

E-mail: [marojbharati99@gmail.com](mailto:marojbharati99@gmail.com), [vikram.singh@ngbu.edu.in](mailto:vikram.singh@ngbu.edu.in), [ram\\_kripal2001@rediffmail.com](mailto:ram_kripal2001@rediffmail.com)

---

## Abstract

The superposition model is utilized to evaluate the crystal field and zero field splitting parameters of single crystals of  $\text{Cr}^{3+}$  doped KZnCST ( $\text{KZnClSO}_4 \cdot 3\text{H}_2\text{O}$ ). Different sites for  $\text{Cr}^{3+}$  ions in KZnCST with distortion are employed for calculation. The zero field splitting parameters that are obtained theoretically with local distortion agree quite well with the experimental values. The optical energy levels for  $\text{Cr}^{3+}$  in KZnCST are established with the Crystal Field Analysis Program and crystal field parameters. The findings indicate that in KZnCST single crystals, one  $\text{Zn}^{2+}$  ion is substituted by a  $\text{Cr}^{3+}$  ion.

**Keywords:**  $\text{Cr}^{3+}$  ions in KZnCST; Crystal field; Optical spectroscopy; Superposition model; Zero-field splitting.

---

Date of Submission: 14-06-2024

Date of acceptance: 28-06-2024

---

## I. Introduction

One useful method for determining the local site symmetry of transition ions in crystals is electron paramagnetic resonance, or EPR. Additionally, it is employed in the identification and characterization of the defects in doped crystals that cause charge compensation [1]. The  $\text{Cr}^{3+}$  ion doped into several crystals provides sufficient information regarding the crystal field (CF) and zero field splitting (ZFS) parameters [2-6]. Doped impurities resulting small structural change influence the crystal's optical qualities. ZFS and CF parameters are primarily determined theoretically using the Superposition Model (SPM) [7-9].

The Zn analogue of  $\text{KMgClSO}_4 \cdot 3\text{H}_2\text{O}$  single crystals used in the fertilizer industry is called KZnCST [10]. It also falls under the group of mineral salts that are utilized as catalysts in a variety of chemical reactions, such as zeolites and antigorite [11, 12].

Studies of optical absorption and EPR have been conducted on  $\text{Cr}^{3+}$  ion doped KZnCST single crystals to determine the characteristics of the crystal field surrounding the  $\text{Cr}^{3+}$  ion and spin Hamiltonian parameters [10]. The ionic radius of  $\text{Zn}^{2+}$  ion (0.074 nm) is slightly larger than that of the  $\text{Cr}^{3+}$  ion (0.0615 nm). Therefore  $\text{Cr}^{3+}$  ion substitutes for one of the  $\text{Zn}^{2+}$  ions as reported in [10].

The modified crystallographic axes (a, b, and c\*) and the laboratory axes (x, y, and z) are chosen in parallel. The labels (X, Y, Z) represent the symmetry adopted axes (magnetic axes). The crystallographic a axis is found to correspond with the principal Z axis of the g and D tensors of  $\text{Cr}^{3+}$  ions.

The superposition model (SPM) analysis of the ZFS and CF parameters for  $\text{Cr}^{3+}$  ions in KZnCST single crystal is presented in this work. The objective is to know the ZFS parameters, the lattice distortion and the CF parameters for the  $\text{Cr}^{3+}$  ions in KZnCST at octahedral sites. The optical energy levels for  $\text{Cr}^{3+}$  ions in KZnCST are computed using CF parameters and Crystal Field Analysis (CFA) computer program. The determined ZFS and CF parameters could be helpful in upcoming research for crystal searches related to a range of scientific and commercial applications.

## II. Crystal structure

KZnCST, which is the Zn equivalent of KMgCST ( $\text{KMgClSO}_4 \cdot 3\text{H}_2\text{O}$ ), crystallizes in a monoclinic system with  $Z = 16$  and space group C2/m. The parameters of the unit cell are as follows:  $\beta = 94^\circ 55'$ ,  $b = 16.23 \text{ \AA}$ ,  $c = 9.53 \text{ \AA}$ , and  $a = 19.72 \text{ \AA}$  [13]. Along the b-axis, a lattice is made up of four chains:  $(\text{SO}_4)_2\text{-Zn}(\text{H}_2\text{O})_2\text{-(H}_2\text{O)}_2\text{-Zn}(\text{H}_2\text{O})_2\text{-(SO}_4)_2$ —the mirror plane containing the  $\text{SO}_4$  tetrahedra. The chains are present on the cell's (0 1 0) cross-section. The chains are held vertically together by  $\text{K}^+$  and  $\text{Cl}^-$  ions. The asymmetric portion of the unit cell contains two Zn atoms. Figure 1 depicts the KZnCST crystal structure along with the symmetry-adopted axis system (SAAS).

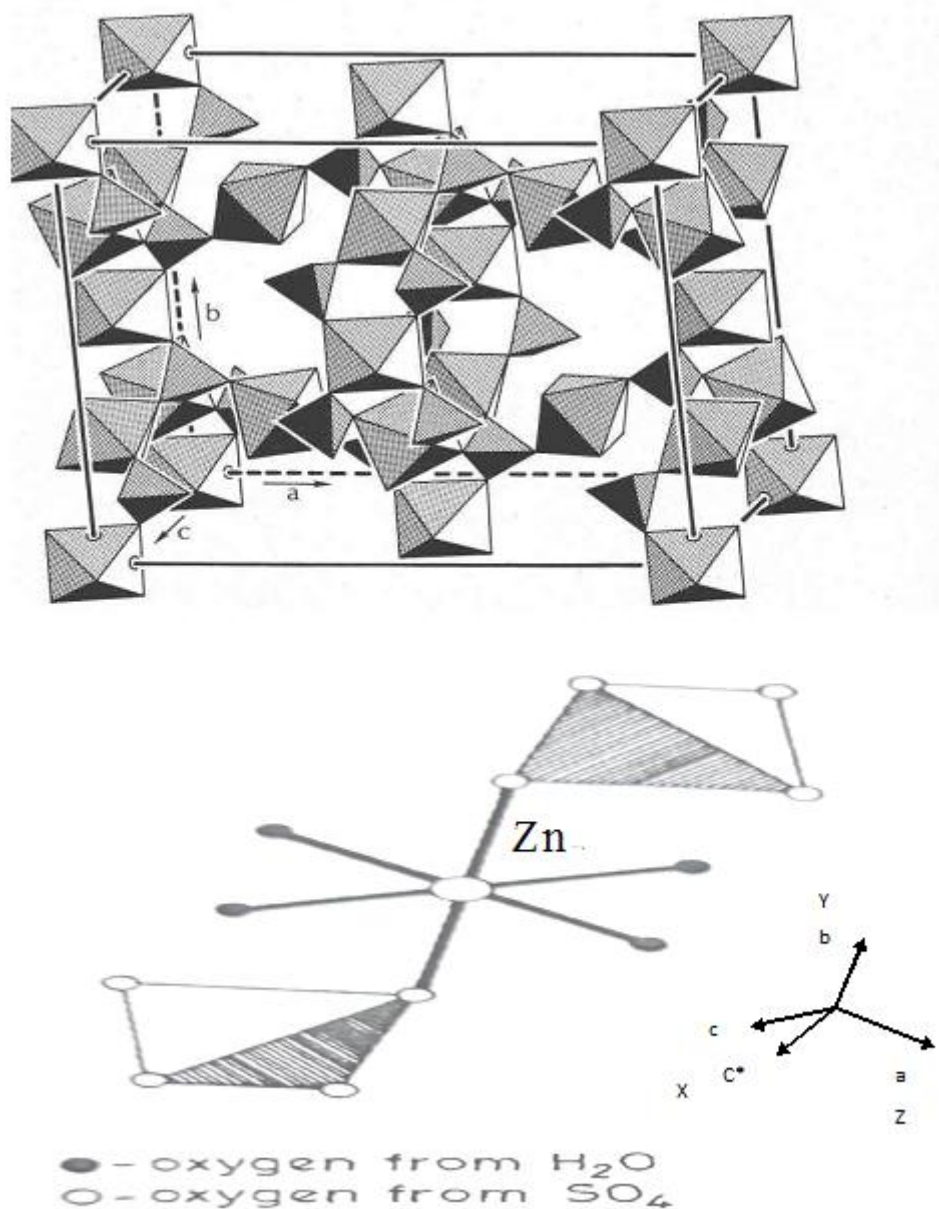


Fig.1. KZnCST crystal structure with the symmetry adopted axis system (SAAS).

The directions of metal-ligand bonds that are mutually perpendicular are the symmetry adopted axes (SAA) or local site symmetry axes. The two other axes (X, Y) are perpendicular to the Z axis for centers I, and the Z axis of SAAS is along the metal-ligand bond Zn-O (crystal *a*-axis) (Fig. 1). This implies that  $\text{Cr}^{3+}$  with roughly orthorhombic symmetry replaces  $\text{Zn}^{2+}$  in the KZnCST crystal. The ionic radius  $\text{Cr}^{3+}$  ion (0.0615 nm) is marginally smaller than  $\text{Zn}^{2+}$  ionic radius (0.074 nm), indicating that  $\text{Cr}^{3+}$  ion can substitute  $\text{Zn}^{2+}$  with certain distortion.

Table 1 lists the spherical polar coordinates of ligands and  $\text{Cr}^{3+}$  ion position for center I in KZnCST[13]. These data are used in KZnCST to compute ZFS and CF for  $\text{Cr}^{3+}$  ions.

### III. Calculations of Splitting Parameters for Zero Field

The following spin Hamiltonian is utilized to ascertain the energy states of  $\text{Cr}^{3+}$  ions within crystals [14, 15, 16]:

$$\mathcal{H} = \mathcal{H}_{Ze} + \mathcal{H}_{ZFS} = \mu_B B \cdot g \cdot S + \sum B_k^q O_k^q = \mu_B B \cdot g \cdot S + \sum f_k b_k^q O_k^q, \quad (1)$$

where the constant magnetic field, Bohr magneton, and spectroscopic splitting factor are represented by the letters  $B$ ,  $\mu_B$ , and  $g$ , respectively.  $S$  presents the effective spin operator and  $O_k^q(S_x, S_y, S_z)$  are the extended Stevens operators (ESO) [17, 18];  $B_k^q$  and  $b_k^q$  are the parameters of ZFS,  $f_k = 1/3$  and  $1/60$  the scaling factors for  $k = 2$  and  $4$ , respectively. For the  $\text{Cr}^{3+}$  ion ( $S = 3/2$ ) at orthorhombic symmetry sites, the ZFS terms in (1) are determined as [19, 20]:

**Table 1.** The spherical polar co-ordinates ( $R, \theta, \phi$ ) of ligands and the  $\text{Cr}^{3+}$  ion's fractional coordinates (center I) in single crystal of KZnCST.

Position of $\text{Cr}^{3+}$	Ligands	Spherical polar coordinates of ligands		
		$R^{\text{\AA}}$	$\theta^{\circ}$	$\phi^{\circ}$
ND: Substitutional (0.0000, 0.0000, 0.0000)	O1	9.4911	23.23	20.40
	O2	5.9749	48.65	72.31
	Ow1	2.1728	15.50	1.18
	Ow2	10.6079	49.75	87.31
	Ow3	7.7182	59.74	33.67
	Ow4	6.0005	76.52	84.99
WD: substitutional Centre I (0.0979, 0.2803, -0.0337)	O1	9.1378	8.27	56.07
	O2	4.3509	11.18	18.25
	Ow1	5.3067	62.93	75.84
	Ow2	8.2766	29.89	-66.51
	Ow3	6.9472	20.08	-37.50
	Ow4	2.6488	49.50	-41.90

ND = No distortion, WD = With distortion.

$$\mathcal{H}_{\text{ZFS}} = B_2^0 O_2^0 + B_2^2 O_2^2 = \frac{1}{3} b_2^0 O_2^0 + \frac{1}{3} b_2^2 O_2^2 = D(S_z^2 - \frac{1}{3} S(S+1)) + E(S_x^2 - S_y^2), \quad (2)$$

The traditional orthorhombic ZFS parameters  $D$ ,  $E$  and  $B_k^q$ ,  $b_k^q$  have the following relations:

$$b_2^0 = D = 3 B_2^0, \quad b_2^2 = 3E = 3 B_2^2. \quad (3)$$

For ZFS, the parameters (in ESO notation) in any symmetry utilizing SPM [19-20] are found as:

$$b_k^q = \sum_i \bar{b}_k(R_0) \left( \frac{R_0}{R_i} \right)^{t_k} K_k^q(\theta_i, \varphi_i), \quad (4)$$

where  $(R_i, \theta_i, \varphi_i)$  present the  $i$ -th ligand's spherical polar coordinates. The intrinsic parameters  $\bar{b}_k$  represent the magnitude of a ligand's  $k$ -th rank ZFS contribution at a distance  $R_i$  and the coordination factors  $K_k^q$  give the geometrical data.  $K_k^q$  for  $k = 1$  to 6 in ESO notation [21] are given in Appendix A1 of [22].

Eq. (4) establishes traditional ZFS parameters,  $D$  and  $E$  in terms of the intrinsic parameters  $\bar{b}_k$ , the power-law exponents  $t_k$  and the reference distance  $R_0$ , as given below [22,23-25]:

$$b_2^0 = D = \frac{\bar{b}_2(R_0)}{2} \left[ \left( \frac{R_0}{R_i} \right)^{t_2} \sum_i (3 \cos^2 \theta_i - 1) \right] \quad (5)$$

$$b_2^2 = 3E = \frac{b_2^2}{3} = \frac{\bar{b}_2(R_0)}{2} \left[ \left( \frac{R_0}{R_i} \right)^{t_2} \sum_i \sin^2 \theta_i \cos 2\varphi_i \right]$$

It is believed that the  $\text{Cr}^{3+}$  ion in KZnCST is substituted at the  $\text{Zn}^{2+}$  ion site and the interstitial site with a ligand environment that is similar. In KZnCST, the local symmetry of the  $\text{Cr}^{3+}$  ion is orthorhombic. In  $\text{LiNbO}_3$  having octahedral coordination of  $\text{Cr}^{3+}$  ion and  $\text{Cr}^{3+}\text{-O}^{2-}$  bond,  $\bar{b}_2(R_0) = 2.34 \text{ cm}^{-1}$  and  $t_2 = -0.12$  [26] were taken to compute  $b_2^0$  and  $b_2^2$ . Given that the  $\text{Cr}^{3+}$  ion in KZnCST has distorted octahedral coordination (Fig. 1), oxygens functioning as ligands, the  $b_k^q$  for center I in the present study are estimated using  $\bar{b}_2(R_0) = 2.34 \text{ cm}^{-1}$  and  $t_2 = -0.96$ .

The spherical polar coordinates of ligands and the  $\text{Cr}^{3+}$  ion's location as listed in Table 1 are employed in the computation. In KZnCST single crystal, the conventional ZFS parameters,  $D$  and  $E$  of the  $\text{Cr}^{3+}$  ion, are determined using Eq. (5). The reference distance  $R_0 = 0.200 \text{ nm}$  is used [27] to yield the ZFS parameters, and the values are:  $|D| = 930.9 \times 10^{-4} \text{ cm}^{-1}$  and  $|E| = 797.3 \times 10^{-4} \text{ cm}^{-1}$  for center I. For symmetry that is orthorhombic, the ratio  $b_2^2 / b_2^0$  should fall between 0 and 1 [28]. In the present calculation, the ratio  $|b_2^2| / |b_2^0| = 2.569$  and  $|E| / |D| = 0.856$  for center I. It is discovered that the calculated values of  $|D|$  and  $|E|$  do not match with the experimental ones and  $|b_2^2| / |b_2^0|$  also does not fall in the specified range [28]. Hence, with above  $t_2$  and reference distance  $R_0$ , the ZFS parameters  $|D|$  and  $|E|$  are calculated for  $\text{Cr}^{3+}$  at the  $\text{Zn}^{2+}$  site with distortion having position  $\text{Zn}^{2+}(0.0979, 0.2803, -0.0337)$  for center I. The local environment about  $\text{Cr}^{3+}$  ion is displayed in Fig. 2. The traditional ZFS parameters estimated now are  $|D| = 1719.1 \times 10^{-4} \text{ cm}^{-1}$ ,  $|E| = 261.0 \times 10^{-4} \text{ cm}^{-1}$  for center I, which match well with the values of the experiment. The ratio  $|b_2^2| / |b_2^0| = 0.455$  and  $|E| / |D| = 0.152$  for center I fall in the specified range [29]. Further, with above  $t_2$  and reference distance  $R_0$ , the ZFS parameters  $|D|$  and  $|E|$  are computed for  $\text{Cr}^{3+}$  at the interstitial site but the values determined are largely different from the experimental ones and for this reason, they are not presented here.

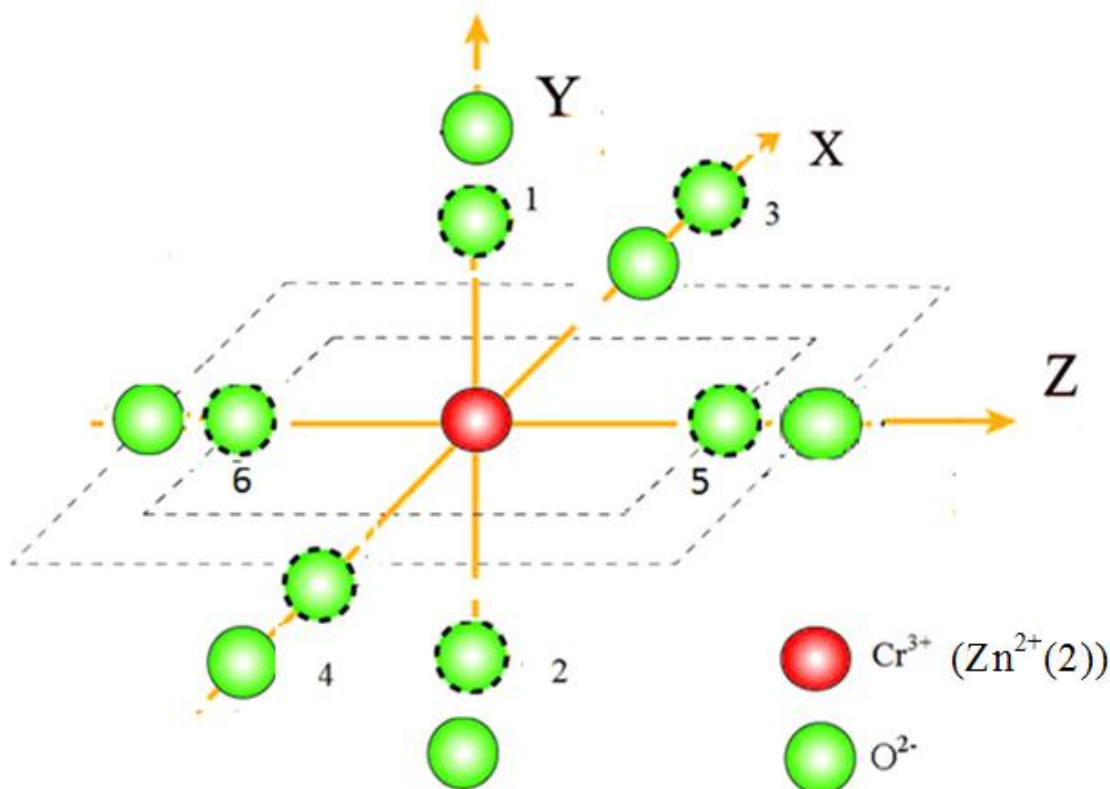


Fig. 2. Graphical presentation of local environment (dotted circles show positions after distortion).

Table 2 shows the experimental and calculated ZFS parameters of the  $\text{Cr}^{3+}$  ion in KZnCST. It is noted from Table 2 that the ZFS parameters  $|D|$  and  $|E|$  are in good agreement with the values of the experiment [10] when the distortion is included into calculation.

**Table 2.** ZFS parameters of  $\text{Cr}^{3+}$  in KZnCST single crystal for center I, both experimentally determined and calculated, along with the reference distance.

Site	$R, \text{\AA}$	Conventional ZFS					
		Calculated ZFS parameters ( $\text{cm}^{-1}$ )			parameters ( $10^{-4}\text{cm}^{-1}$ )		
		$ b_2^0 $	$ b_2^2 $	$ b_2^2 / b_2^0 $	$ D $	$ E $	$ E / D $
ND	2.00	0.09309	0.23919	2.569	930.9	797.3	0.856
Center I							
WD	2.00	0.17191	0.07831	0.455	1719.1	261.0	0.152
					1719.0 <sup>e</sup>	261.0 <sup>e</sup>	0.152

WD = With distortion, ND = No distortion, <sup>e</sup> = experimental.

#### IV. Calculations of the Crystal Field Parameters

The transition ion CF energy states in crystals [29–32] can be determined using Wybourne operators as [14, 33, 34]:

$$\mathcal{H}_{\text{CF}} = \sum_{kq} B_{kq} C_q^{(k)} \quad (6)$$

where  $\mathcal{H}_{\text{CF}}$  is CF Hamiltonian. The metal-ligand complex's CF parameters in equation (6) are established using SPM [19-20] as given below:

$$B_{kq} = \sum_i \bar{A}_k \left( \frac{R_0}{R_i} \right)^{t_k} K_{kq}(\theta_i, \varphi_i). \quad (7)$$

$R_0$  represents the reference distance,  $R_i$ ,  $\theta_i$ ,  $\varphi_i$  give the  $i^{\text{th}}$  ligand's spherical polar coordinates and  $K_{kq}$  are the coordination factors [29]. To obtain  $B_{kq}$  ( $k = 2, 4$ ;  $q = 0, 2, 4$ ) the following values are taken:  $\bar{A}_2 = 40, 400 \text{ cm}^{-1}$ ,

$t_2 = 1.3$ ,  $\bar{A}_4 = 11, 700 \text{ cm}^{-1}$  and  $t_4 = 3.4$  [29]. The  $B_{kq}$  parameters evaluated are given in Table 3. For center I, the ratio  $|B_{22}|/|B_{20}| = 0.353$  demonstrates that the established  $B_{kq}$  parameters are standardized [28]. By diagonalizing the total Hamiltonian and using the  $B_{kq}$  parameters in Table 3 and the CFA computer program [30, 31], the CF energy levels of the  $\text{Cr}^{3+}$  ion in KZnCST single crystals are determined. The calculated energy values are shown in Table 4. For  $\text{Cr}^{3+}$ : KZnCST, the calculated and experimental energy values are contrasted [10]. The experimental and theoretical energy values appear to be in a fair amount of agreement, as Table 4 shows. Hence, the experimental results are supported by the examination of  $\text{Cr}^{3+}$  ions at  $\text{Zn}^{2+}$  sites theoretically in KZnCST [10].

**Table 3.**  $B_{kq}$  parameters of  $\text{Cr}^{3+}$  for center I with distortion in a single crystal of KZnCST.

Calculated $B_{kq}$ ( $\text{cm}^{-1}$ ) Parameters used for CFA program							
Site	$R_0^{\text{\AA}}$	$B_{20}$	$B_{22}$	$B_{40}$	$B_{42}$	$B_{44}$	$ B_{22} / B_{20} $
Center I							
WD	2.00	24311.49	-8594.43	-14664.1	1198.291	-7246.45	0.353

WD = With distortion.

The spectra of optical absorption of  $\text{Cr}^{3+}$ -activated phosphors are currently explained using Franck-Condon analysis with configurational-coordinate (CC) model [35]. The various excited state-ground state transitions in  $\text{Cr}^{3+}$  are a result of strong coupling (CC model) of the lattice vibrations [35]. The CC model is not being considered and hence there is difference between excited-state peak energies found here and energies of the zero-phonon line (ZPL) described in [35, 36]. Two groups of oxide-phosphors doped with  $\text{Cr}^{3+}$  are taken up: (i) O-Cr-A type, (ii) O-Cr-B type. The luminescence properties of type (i) phosphors are obtained from the  ${}^2\text{E}_g$ -related luminescence transitions as their crystal-field strength falls in the region of  $Dq/B > 2.1$  while type (ii) phosphors have a crystal-field strength lying within the range of  $Dq/B < 2.1$ , hence, the optical transitions associated with  ${}^4\text{T}_{2g}$  are utilized to find their luminescence properties. KZnCST:  $\text{Cr}^{3+}$  falls under (i) type phosphors ( $Dq/B = 2.38$  which is  $> 2.1$ ) [36].

#### V. Summary and Conclusions

For  $\text{Cr}^{3+}$  ions in KZnCST single crystals, the zero-field splitting (ZFS) and crystal field (CF) parameters are computed using the superposition model (SPM). Calculations are performed using  $\text{Cr}^{3+}$  ions in KZnCST crystal at the  $\text{Zn}^{2+}$  ion sites, interstitial site, and distortion models. When distortion is taken into account, the calculated conventional ZFS values for the  $\text{Cr}^{3+}$  ion at  $\text{Zn}^{2+}$  sites in KZnCST single crystal show

good agreement with the experimental values. The  $\text{Cr}^{3+}$  ions are established to be substituted at  $\text{Zn}^{2+}$  ion sites in KZnCST. The CF energy values for  $\text{Cr}^{3+}$  ions at  $\text{Zn}^{2+}$  sites evaluated with CFA program and CF parameters present a reasonable agreement with the experimental ones. So, the theoretical inferences validate the experimental conclusion.

**Table 4.** Energy values found through experimentation and computation (center I) of  $\text{Cr}^{3+}$  in KZnCST single crystal.

Transition from $^4A_{2g}(F)$ state	Observed band ( $\text{cm}^{-1}$ )	Calculated band from CFA ( $\text{cm}^{-1}$ ) Center I
$^2E_g(G)$	11975	10388, 11521
$^2T_{1g}(G)$		12161, 12418, 12485
$^4T_{2g}(F)$	17235	15396, 16932, 16978, 17354, 17925, 18716
$^4T_{1g}(F)$	24385	19759, 20876, 21866, 23380, 23834, 24744
$^4T_{1g}(P)$		26175, 26544, 26625, 27045, 27590, 28162
$^2T_{1g}(aD)$		31866, 33603, 34554
$^2E_g(bD)$		34780, 35559

(The spin-orbit coupling constant, Racah parameters A, B, and C, and the Trees correction are 276, 0, 724, 2484, and  $70 \text{ cm}^{-1}$ , respectively)

The modeling procedure used in the current investigation can be helpful in correlating EPR and optical data for many other ion-host systems to obtain crystals of several commercial and scientific applications.

### Acknowledgement

The authors are grateful to Prof. C. Rudowicz of the Faculty of Chemistry at A. Mickiewicz University in Poznan, Poland, for providing the CFA computer program, and to the physics department head for providing departmental facilities.

### References

- [1]. Irmscher K, Prokjesch M. Spectroscopic evidence and control of compensating native defects in doped ZnSe. *Mater. Sci. Eng. B* 2001; 80: 168-172.
- [2]. Stefaniuk I, Rudowicz C, Gnutek P, Suchocki A. EPR Study of  $\text{Cr}^{3+}$  and  $\text{Fe}^{3+}$  Impurity Ions in Nominally Pure and  $\text{Co}^{2+}$ -Doped  $\text{YAlO}_3$  Single Crystals. *Appl. Magn. Reson.* (2009) 36:371-380.
- [3]. Mabbs F E, Collison D, Gatteschi D. *Electron Paramagnetic Resonance of d Transition Metal Compounds*, Amsterdam: Elsevier; 1992.
- [4]. Weil J A, Bolton J R. *Electron Paramagnetic Resonance: Elementary Theory and Practical Applications*, 2nd ed., New York: Wiley; 2007.
- [5]. Pilbrow J R. in: *Transition Ion Electron Paramagnetic Resonance*, Oxford: Clarendon Press; 1990.
- [6]. Bansal R S, Seth V P, Chand P, Gupta S K. EPR and optical spectra of vanadyl ion (impurities) in three polycrystalline solids. *J. Phys. Chem. Solids* 1991; 52: 389-392.
- [7]. Brik M G, Avram C N, Avram N M. Calculations of spin Hamiltonian parameters and analysis of trigonal distortions in  $\text{LiSr}(\text{Al}, \text{Ga})\text{F}_6:\text{Cr}^{3+}$  crystals. *Physica B*. 2006; 384: 78-81. doi.org/10.1016/j.physb.2006.05.155.
- [8]. Pandey S, Kripal R, Yadav A K, Açıkgoz M, Gnutek P, Rudowicz C. Implications of direct conversions of crystal field parameters into zero-field splitting ones - Case study: Superposition model analysis for  $\text{Cr}^{3+}$  ions at orthorhombic sites in  $\text{LiKSO}_4$ . *J. Lumin.* 2021; 230: 117548 (10 pages).
- [9]. Bradbury M I, Newman D J. Ratios of crystal field parameters in rare earth salts. *Chem. Phys. Lett.* 1967; 1: 44-45. doi.org/10.1016/0009-2614(67)80063-0.
- [10]. B. Deva Prasad Raju, J. Lakshmana Rao, K. V. Narasimulu, N. O. Gopal, C. S. Sunandana, EPR and optical absorption studies on  $\text{Cr}^{3+}$  ions doped in  $\text{KZnClSO}_4 \cdot 3\text{H}_2\text{O}$  single crystals, *Spectrochimica Acta Part A* 61 (2005) 2195-2198.
- [11]. Martin-Luengo M A, Yates M. Zeolitic materials as catalysts for organic syntheses. *J. Mater. Sci.* 1995; 30: 4483-4491.
- [12]. Reddy S N, Ravikumar R V S S N, Reddy B J, Reddy Y P, Rao P S. Spectroscopic investigations on  $\text{Fe}^{3+}$ ,  $\text{Fe}^{2+}$  and  $\text{Mn}^{2+}$  bearing antigorite mineral. *Neues Jahrbuch Fur Mineralogie-Monatshefte* 2001; 6: 261.
- [13]. Robinson P D, Fang J H, Ohya Y. The Crystal Structure of Kainite. *Am. Min.* 1972; 57: 1325-1332.

- [14]. Rudowicz C, Karbowiak M. Disentangling intricate web of interrelated notions at the interface between the physical (crystal field) Hamiltonians and the effective (spin) Hamiltonians. *Coord. Chem. Rev.* 2015;287: 28-63.
- [15]. Rudowicz C. Concept of spin Hamiltonian, forms of zero field splitting and electronic Zeeman Hamiltonians and relations between parameters used in EPR. A critical review. *Magn. Reson. Rev.* 1987;13: 1-89; Erratum, Rudowicz C. *Magn. Reson. Rev.* 1988;13: 335.
- [16]. Rudowicz C, Misra SK. Spin-Hamiltonian formalisms in electron magnetic resonance (EMR) and related spectroscopies. *Appl. Spectrosc. Rev.* 2001;36(1):11-63.
- [17]. Rudowicz C. Transformation relations for the conventional  $O_k^q$  and normalised  $O_k^q$  Stevens operator equivalents with  $k=1$  to 6 and  $-k \leq q \leq k$ . *J. Phys. C Solid State Phys.* 1985;18( 7): 1415-1430; Erratum: Rudowicz C. *J. Phys. C Solid State Phys.* 1985;18(19): 3837.
- [18]. Rudowicz C, Chung C Y. The generalization of the extended Stevens operators to higher ranks and spins, and a systematic review of the tables of the tensor operators and their matrix elements. *J. Phys. Condens. Matter* 2004;16(32): 5825-5847.
- [19]. Newman D J, Ng B. Superposition model. Ch. 5 in: Newman D J, Ng B. (Eds.). *Crystal Field Handbook*. UK: Cambridge University Press; pp. 83–119, 2000.
- [20]. Newman D J, Ng B. The Superposition model of crystal fields. *Rep. Prog. Phys.* 1989;52:699-763.
- [21]. Rudowicz C. On the derivation of the superposition-model formulae using the transformation relations for the Stevens operators. *J. Phys. C: Solid State Phys.* 1987; 20(35):6033-6037.
- [22]. Rudowicz C, Gnutek P, Açıkgöz M. Superposition model in electron magnetic resonance spectroscopy – a primer for experimentalists with illustrative applications and literature database. *Appl. Spectroscopy Rev.* 2019;54: 673-718.
- [23]. Açıkgöz M. A study of the impurity structure for  $3d^3$  ( $\text{Cr}^{3+}$  and  $\text{Mn}^{4+}$ ) ions doped into rutile  $\text{TiO}_2$  crystal. *Spectrochim. Acta A* 2012;86(2): 417-422.
- [24]. Müller KA, Berlinger W, Albers J. Paramagnetic resonance and local position of  $\text{Cr}^{3+}$  in ferroelectric  $\text{BaTiO}_3$ . *Phys. Rev. B* 1985; 32(9): 5837-5850.
- [25]. Müller KA, Berlinger W. Superposition model for sixfold-coordinated  $\text{Cr}^{3+}$  in oxide crystals (EPR study). *J. Phys. C: Solid State Phys.* 1983;16(35):6861-6874.
- [26]. Yeom T H, Chang Y M, Rudowicz C.  $\text{Cr}^{3+}$  centres in  $\text{LiNbO}_3$ : Experimental and theoretical investigation of spin Hamiltonian parameters. *Solid State Commun.* 1993; 87(3):245-249.
- [27]. Siegel E, Muller K A. Structure of transition-metal—oxygen-vacancy pair centers. *Phys. Rev. B* 1979;19(1):109-120.
- [28]. Rudowicz C, Bramley R. On standardization of the spin Hamiltonian and the ligand field Hamiltonian for orthorhombic symmetry. *J. Chem. Phys.* 1985; 83(10):5192-5197.
- [29]. Yeung YY, Newman D J. Superposition-model analyses for the  $\text{Cr}^{3+4}\text{A}_2$  ground state. *Phys. Rev. B* 1986; 34(4):2258-2265.
- [30]. Yeung YY, Rudowicz C. Ligand field analysis of the  $3d^N$  ions at orthorhombic or higher symmetry sites. *Comp. Chem.* 1992; 16(3):207-216.
- [31]. Yeung YY, Rudowicz C. Crystal Field Energy Levels and State Vectors for the  $3d^N$  Ions at Orthorhombic or Higher Symmetry Sites. *J. Comput. Phys.* 1993;109(1):150-152.
- [32]. Chang Y M, Rudowicz C, Yeung YY. Crystal field analysis of the  $3d^N$  ions at low symmetry sites including the ‘imaginary’ terms. *Computers in Physics* 1994;8(5):583-588.
- [33]. Wybourne B G. *Spectroscopic Properties of Rare Earth*. New York, USA: Wiley; 1965.
- [34]. Figgis B N, Hitchman M A. *Ligand Field Theory and its Applications*. New York: Wiley; 2000.
- [35]. Adachi S. Photoluminescence Spectroscopy and Crystal-Field Parameters of  $\text{Cr}^{3+}$  Ion in Red and Deep Red-Emitting Phosphors. *ECS J Solid State Sci. Tech.* 2019;8 (12): R164-R168.
- [36]. Adachi S. Review—Photoluminescence Properties of  $\text{Cr}^{3+}$ -Activated Oxide Phosphors. *ECS J Solid State Sci. Tech.* 2021;10: 026001(21 pages).

## Declarations:

### Ethical Approval:

This research did not contain any studies involving animal or human participants, nor did it take place on any private or protected areas. No specific permissions were required for corresponding locations.

### Competing interests:

The authors declare that they have no known competing financial interests or personal relationships that could have appeared to influence the work reported in this paper.

### Authors' contributions:

Maroj Bharati and Vikram Singh- performed calculations, wrote the manuscript and prepared the figure.

Ram Kripal- idea and supervision.

All authors have reviewed the manuscript.

### Funding:

No funding is received.

### Availability of data and materials:

The data will be made available on request.